Anisotropic Phases of Superfluid ^{3}He in Compressed Aerogel

J. I. A. Li,* A. M. Zimmerman, J. Pollanen,‡ C. A. Collett, and W. P. Halperin†
Northwestern University, Evanston, Illinois 60208, USA
(Received 30 October 2014; published 10 March 2015)

It has been shown that the relative stabilities of various superfluid states of ^{3}He can be influenced by anisotropy in a silica aerogel framework. We prepared a suite of aerogel samples compressed up to 30% for which we performed pulsed NMR on ^{3}He imbibed within the aerogel. We identified A and B phases and determined their magnetic field-temperature phase diagrams as a function of strain. From these results, we infer that the B phase is distorted by negative strain forming an anisotropic superfluid state more stable than the A phase.

DOI: 10.1103/PhysRevLett.114.105302 PACS numbers: 67.30.hm, 67.30.er

The A and B phases of superfluid ^{3}He are unconventional Cooper paired states with orbital angular momentum $L = 1$. They are just two of many p-wave states, each distinguished by unique broken symmetries, and these are the only stable states in pure ^{3}He in low magnetic field [1]. However, new phases in this manifold have been reported for superfluid confined within an anisotropic external framework; in one case, chiral states within positively strained 98% porous, silica aerogel [2] and in another, equal spin pairing states within nematically oriented alumina hydrate aerogels [3]. Additionally, for a negatively strained aerogel, obtained by compression, we found that the relative thermodynamic stability between the A and B phases can be reversed resulting in an unusual tricritical point between A, B, and normal phases with a critical magnetic field of $H_c \approx 100$ mT [4].

Our observation of preferential B-phase stability relative to the A phase [4] appears at first glance to be inconsistent with theoretical predictions where it was established that anisotropic scattering of ^{3}He quasiparticles would favor the anisotropic A phase, over the isotropic B phase [5–7]. To address this problem, we have investigated the dependence of the A-to-B phase diagram as a function of negative strain.

Here, we report that the square of this critical field is directly proportional to the aerogel anisotropy, which we determined from optical birefringence. Based on our measurements of the strain dependence of the A-to-B phase diagram, we have determined that the B-phase entropy is increased relative to the unstrained B phase which transforms under negative strain to a new type of anisotropic superfluid, which we call a distorted B phase, that can effectively compete with the A phase in a magnetic field.

We prepared two different batches of aerogel samples of 98% porosity, batch **a** and **b**, in the shape of cylinders 4.0 mm in diameter with unstrained length of 5.1 mm. For clarity, we label the sample by the batch number as well as the nominal amount of negative strain introduced by compression; e.g., a sample from batch **a** with −19.4% negative strain is labeled as sample **a19**. Some results with samples from batch **a** have also been reported previously [4,8–10], where the superfluid phases were identified and the amplitude of the order parameter was measured. A critical field was discovered for samples with negative strain −19.4% (**a19**) and −22.5%(**a23**) introduced into isotropic samples from the same batch (**a0**); **a19** (originally **a0**) was measured with the strain axis parallel to the magnetic field, $\boldsymbol{\epsilon} \| \mathbf{H}$, and **a23** with $\boldsymbol{\epsilon} \perp \mathbf{H}$. In the present Letter, three new samples are taken from batch **b** prepared using the same methods as batch **a**. Optical birefringence was performed before introducing anisotropy by compression and the samples were found to be homogeneous and isotropic, Fig. 1(a) [11,12]. We strained these samples −11.7% (**b12**), −19.8% (**b20**), and −30.0% (**b30**) by mechanical compression measured as a displacement at room temperature. The strain induced anisotropy was characterized by the intensity from transmitted optical birefringence, Figs. 1(b)–1(d), taken from a 2×2 mm^2 central portion of the images. The integrated intensity as a function of strain for the two different batches are consistent with each other, Fig. 1(e), both of which show a delayed onset of birefringence with strain of $\boldsymbol{\epsilon} \approx -8\%$, due to the intrinsic mechanical behavior of the aerogel (see Supplemental Material [13]). Beyond this onset, the transmitted intensity increases linearly. All **b** samples were oriented with the strain axis parallel to the field, cooled simultaneously, and filled with ^{3}He supercritically. We performed pulsed NMR measurements at a pressure $P = 26.5$ bar in magnetic fields ranging from $H = 49.1$ to 214 mT with small tip angles, $\beta \sim 20°$. Detailed procedures for these measurements and their analyses have been described earlier [2,8,10].

The field dependence of the thermodynamic transitions on warming, $T_{BA}(H^2)$ are shown in Fig. 2 for sample **a0**, **b12**, **b20**, and **b30**. Quadratic field dependencies are observed for the field suppression of T_{BA} in all samples, which can be qualitatively understood by analogy with the free energy difference between A and B phases for pure ^{3}He in the Ginzburg-Landau limit given by,

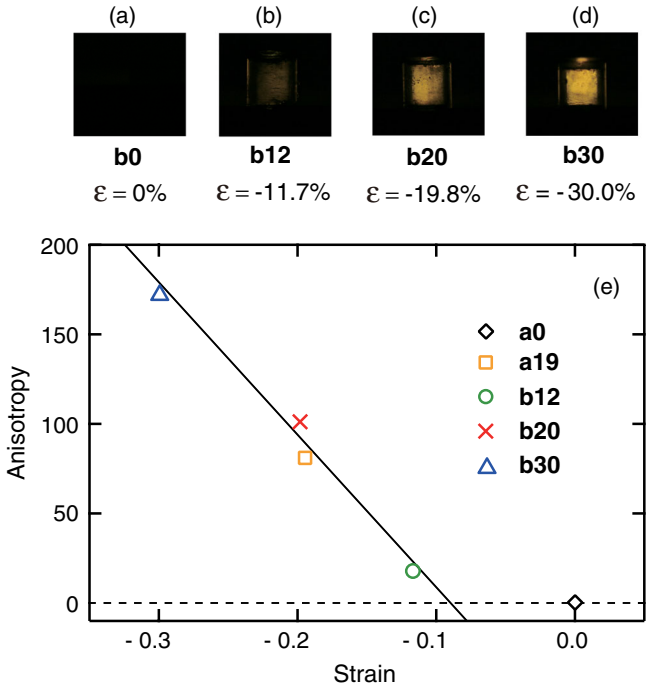

FIG. 1 (color online). Anisotropy introduced by compressive strain, $\boldsymbol{\varepsilon}$, in two batches of 98% porosity aerogel, **a** and **b**. (a) to (d) Optical birefringence images of the transmitted light intensity through the aerogel samples. (e) Anisotropy in the aerogel, defined as the intensity of the optical birefringent signal, versus strain. The black solid line is a linear fit for samples from batch **b**.

$$F_B - F_N = -\frac{1}{36}\frac{[\alpha^2(T) + 2\alpha(T) g_z H^2]}{\beta_{12} + \frac{1}{3}\beta_{345}} + O(H)^4, \quad (1)$$

$$F_A - F_N = -\frac{1}{36}\frac{\alpha^2(T)}{\beta_{245}}. \quad (2)$$

The β_i and g_z are material parameters in the Ginzburg-Landau functional [21,22] that determine the superfluid condensation energy and the symmetry of the superfluid states, and $\alpha(T) \propto 1 - T/T_c$. The B phase has a quadratic field dependent free energy compared to the normal state, whereas the A-phase free energy is field independent. From Eqs. (1) and (2), the field suppression of T_{BA} in the Ginzburg-Landau limit can be written as, [23,24]

$$1 - \frac{T_{BA}}{T_c} = g_{BA}\left(\frac{H^2 - H_c^2}{H_0^2}\right) + O\left(\frac{H}{H_0}\right)^4, \quad (3)$$

where $H_c = 0$ for pure ^{3}He and for ^{3}He in an isotropic aerogel [8]. H_0 and g_{BA} are constants from the Ginzburg-Landau theory [5,25,26]. However, the presence of strain in the aerogel breaks the orbital rotation symmetry of the superfluid to which we attribute the appearance of a critical field, H_c, that we find depends systematically on the magnitude of the strain. In fact, all anisotropic aerogel samples with negative strain exhibit this behavior as exemplified in Fig. 2. The existence of a critical field is indicative of a new term in the relative free energy between the A and B phase which is not captured by Eqs. (1) and (2). To determine the origin of H_c, we must isolate how each of the phases is affected by strain. For this purpose, we measure the longitudinal resonance frequency of the superfluid A and B phases, Ω_A and Ω_B, which are directly related to their respective order parameter amplitudes, Δ_A and Δ_B, and correspondingly, to their free energy.

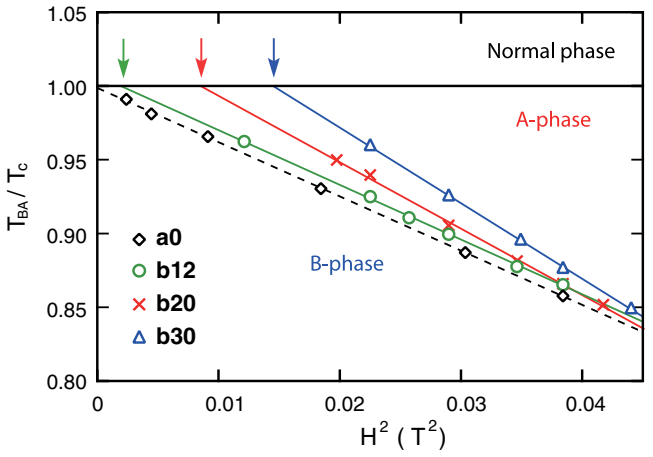

FIG. 2 (color online). Superfluid phase diagram T_{BA}/T_c versus H^2, with $\boldsymbol{\varepsilon} \| \boldsymbol{H}$ for anisotropic **b** samples compared to the isotropic sample **a0** [10] at a pressure of $P = 26.5$ bar from warming experiments. The superfluid transition temperatures, T_c, for **a0**, **b12**, **b20**, and **b30** are 2.213, 2.152, 2.118, and 2.118 mK. The critical fields are indicated by arrows: $H_c = 45.5$ mT, 91.8 mT, and 120.2 mT for these samples.

For the isotropic sample **a0**, Ω_A and Ω_B satisfy the Leggett relation, Eq. (4), which expresses the unique order parameter symmetries of the A and B phases in the Ginzburg-Landau regime given by,

$$\frac{5}{2} = \frac{\Omega_B^2}{\Omega_A^2}\frac{\chi_B}{\chi_A}\frac{\Delta_A^2}{\Delta_B^2}, \quad (4)$$

where we take $\Delta_A^2 \approx \Delta_B^2$ [8,27] [28] and the susceptibilities χ_A and χ_B are measured.

The maximum frequency shift of the A phase from sample **a0** is shown in Fig. 3 as open black diamonds, where the entire sample is in the dipole-locked configuration ($\hat{\boldsymbol{d}} \| \hat{\boldsymbol{l}} \perp \boldsymbol{H}$) ensured by warming from the B phase [10], where $\hat{\boldsymbol{d}}$ is the direction along which the spin projection is zero, and $\hat{\boldsymbol{l}}$ is the direction of the orbital angular momentum. The longitudinal resonance frequency can be calculated from the high field approximation: ${\Omega_A}^2 = 2\omega_L \Delta\omega_A$ with $\Delta\omega_A$ the measured shift in frequency from the Larmor frequency ω_L. When our isotropic aerogel is subjected to sufficient uniaxial negative strain the A phase becomes a two-dimensional (2D) orbital glass phase [4] with frequency shift at small NMR tip angles β given by [30,31],

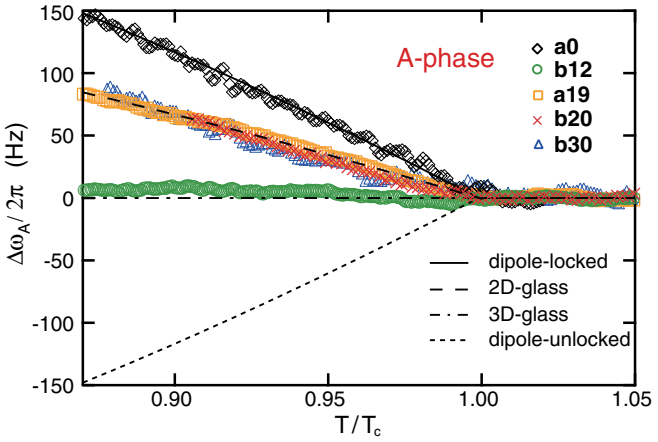

FIG. 3 (color online). NMR frequency shifts of the A phase, $\Delta\omega_A$, as a function of reduced temperature measured with small tip angle, at $P \approx 26$ bar, adjusted to a common field of $H = 196$ mT. On warming from the B phase, sample **a0** is in the dipole-locked ($\hat{\boldsymbol{d}} \| \hat{\boldsymbol{l}} \perp \boldsymbol{H}$) configuration giving a maximum frequency shift (black diamonds) [8]. The black solid curve is for the frequency shift of pure ^{3}He-A with a scaling factor of 0.42, corresponding to an order parameter suppression of 0.35. The frequency shift of a two-dimensional glass phase at small tip angle is calculated using Eq. (5), black dashed curve, in good agreement with the data for **a19** at 174 mT (orange squares) and for **b20** (red crosses) and **b30** (blue triangles) at 196 mT. The negligible shift for **b12** (green circles) with no linewidth increase (not shown), is characteristic of a three-dimensional glass phase [10].

$$\Delta\omega_{2D} = \frac{{\Omega_A}^2}{4\omega_L}, \quad \beta \approx 0. \tag{5}$$

Using Ω_A determined from the isotropic sample **a0** and Eq. (5), the frequency shift for a 2D glass phase with the same order parameter amplitude is plotted as the black dashed curve in Fig. 3. The frequency shift for samples **a19**, **b20**, and **b30**, Fig. 3, agree well with the black dashed curve, showing that the longitudinal resonance frequency of the A phase, Ω_A, is not affected by negative strain up to 30%. We conclude that the order parameter amplitude of the A phase, Δ_A, is insensitive to aerogel anisotropy induced by negative strain and consequently, the free energy is also unaffected. Additionally, a zero frequency shift and zero linewidth increase are observed in sample **b12**, Fig. 3, indicative of the existence of a three-dimensional (3D) glass phase [10]. As shown in Figs. 1(b) and 1(e), sample **b12** is strained significantly by $\boldsymbol{\varepsilon} = -11.7\%$ but only displays a weak optical birefringence due to the delayed onset of anisotropy at $\sim -8\%$ strain. Therefore, the observation of a 3D glass phase suggests a threshold aerogel anisotropy below which the continuous 3D rotational symmetry of the order parameter, and thus the 3D glass phase, is preserved (see Supplemental Material [13]). Consequently, the transition from a 3D-glass phase to a 2D-glass phase must occur with increasing (negative) strain within a small 7% window. The NMR tip angle behavior of the 3D glass phase in sample **b12** is shown in the Supplemental Material [13].

In the B phase, the order parameter texture with orbital quantization axis $\hat{\ell}$ perpendicular to the magnetic field, for example, constrained by sample walls, has a maximum frequency shift for small β directly related to the longitudinal resonance frequency and can be identified as a prominent peak in the spectrum at large frequency [8],

$$\Delta\omega_B = \frac{2}{5}\frac{\Omega_B^2}{\omega_L}, \qquad \beta \approx 0. \tag{6}$$

We refer to the spin dynamics of this texture as the $\hat{\ell} \perp \boldsymbol{H}$ mode. In previous work, we measured $\Delta\omega_B$, for this mode in sample **a0** [8], shown in Fig. 4 together with its extension to T_c as a black dashed curve. When we compare this to the frequency shift in the A phase, Fig. 3, we obtain the factor of $5/2$ given in Eq. (4); this factor expresses the characteristic symmetries of the axial and isotropic p-wave states (A and B phases, respectively) as is the case for pure superfluid ^{3}He. On the other hand, for the negatively strained aerogels **a19** and **a23**, the $\hat{\ell} \perp \boldsymbol{H}$-mode frequency shifts are significantly increased. The black dash-dotted curve is a fit to our data for $H = 95.6$ mT found by multiplying the black dashed curve by 1.7. We conclude that the B phase in

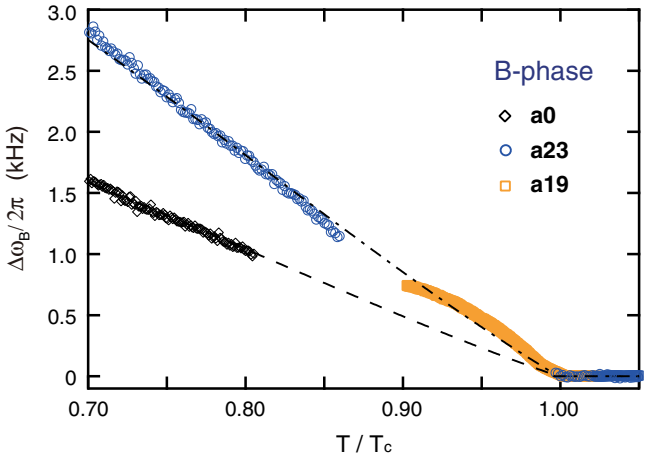

FIG. 4 (color online). NMR frequency shifts $\Delta\omega_B$ of the B phase as a function of reduced temperature measured with small tip angle, at $P = 26.3$ bar. The frequency shifts are from a peak in the NMR spectrum [8] corresponding to the texture, $\hat{\ell} \perp \boldsymbol{H}$, that determines Ω_B, Eq. (6). This texture appears above (below) a crossover temperature $T_x \sim 0.85 T_c$ for sample **a19** (**a23**); see Supplemental Material [13]. The frequency shifts for the anisotropic samples **a19** and **a23**, measured at $H = 95.6$ mT, are significantly larger than for the isotropic sample **a0** indicating a change in the order parameter for strain $\boldsymbol{\varepsilon} \sim -20\%$. The frequency shift for sample **a0** was measured at $H = 196$ mT and scaled to a common field of 95.6 mT using Eq. (6). A comparison with samples **b20** and **b30** was not possible owing to texture inhomogeneity for $T > T_x$.

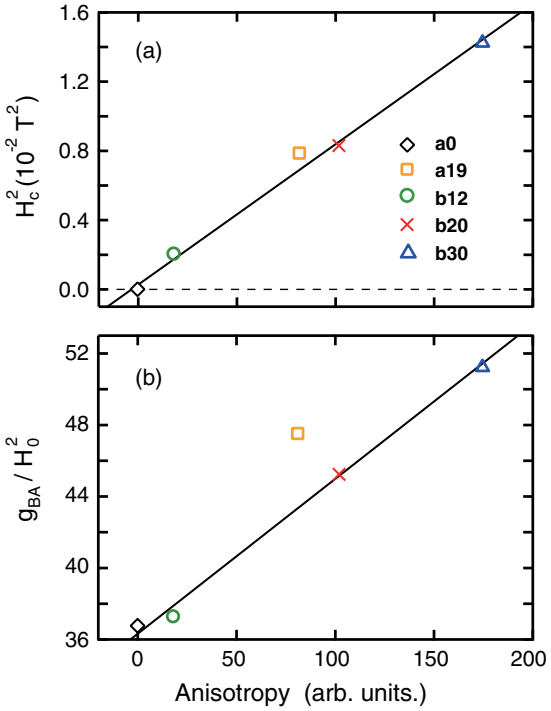

FIG. 5 (color online). (a) The critical field squared H_c^2 and (b) g_{BA}/H_0^2 for sample **a0** (open black diamond), **a19** (open orange square), **b12** (open green circles), **b20** (red crosses), and **b30** (open blue triangles) as a function of aerogel anisotropy taken from measurements of the optical birefringence intensity. ${H_c}^2$, and g_{BA}/H_0^2 show a strict proportionality to aerogel anisotropy, with the exception of sample **a19**. Sample **a19** does not lie on the same line as the batch **b** samples for the second parameter, g_{BA}/H_0^2.

strained aerogel is not an isotropic state and might have a different order parameter symmetry. This is a new type of anisotropic superfluid which continuously evolves from the isotropic B phase with increasing anisotropy induced by the compressive strain in the aerogel.

In Eq. (3), the two parameters affected by strain deduced from the AB-phase diagram are the square of the critical field, H_c^2, and the slope of the B to A-phase transition, g_{BA}/H_0^2. In Fig. 5, we plot these two quantities as a function of anisotropy for the three aerogel **b** samples compared with the isotropic sample **a0** and find that they are proportional to the anisotropy induced by strain. We understand that the mechanism by which strain modifies the superfluid is to create anisotropic quasiparticle scattering in the superfluid. Consequently, we can infer that anisotropic scattering smoothly increases with aerogel anisotropy and is responsible for creating a distorted B phase. Although we have not made a specific identification of the new state it is nonetheless clear from our susceptibility measurements that it is a nonequal spin pairing state (NESP) with the same susceptibility as the B phase. The latter comparison was made between **a19** and in the unstrained aerogel **a0** at the same temperature, pressure, and field on their respective AB-phase boundaries [26] following the procedure described in Refs. [4,8,10].

With this input, we can calculate the change of entropy of the new phase, compared to the isotropic B phase, using the Clausius-Clapeyron equation,

$$\frac{dT}{dH^2} = -\frac{1}{2}\frac{\chi_A - \chi_{\rm new}}{S_A - S_{\rm new}}, \tag{7}$$

where χ and S are the susceptibility and the entropy of the two phases along the phase equilibrium line. Since the slopes of these lines, Fig. 2, are increasingly more negative with increasing strain, we deduce that the new phase has a higher entropy compared with the isotropic aerogel B phase.

In summary, we report NMR measurements as a function of compressive strain in an aerogel that determine the phase diagrams of the superfluid phases within the aerogel framework. The anisotropy in the aerogel stabilizes a new anisotropic nonequal spin pairing superfluid state which evolves continuously from the isotropic B phase with increasing strain. The tricritical point between normal ^{3}He, the A phase, and the distorted B phase is marked by a critical field for which the square of the field is proportional to the anisotropy. Additionally, the entropy of this distorted B phase is larger than that of the isotropic B phase.

We are grateful to J. J. Wiman, J. A. Sauls, V. V. Dmitriev, Yoonseok Lee, J. M. Parpia, and G. E. Volovik for helpful discussion and to W. J. Gannon for help in the early phases of this work and to the National Science Foundation for support, Grant No. DMR-1103625.

*jiali2015@u.northwestern.edu
†w-halperin@northwestern.edu
‡Present address: Institute for Quantum Information and Matter (IQIM), California Institute of Technology, Pasadena, California 91125, USA.

[1] D. Vollhardt and P. Wölfle, *The Superfluid Phases of Helium 3* (Taylor and Francis, London, 1990).
[2] J. Pollanen, J. I. A. Li, C. A. Collett, W. J. Gannon, W. P. Halperin, and J. A. Sauls, Nat. Phys. **8**, 317 (2012).
[3] R. S. Askhadullin, V. V. Dmitriev, D. A. Krasnikhin, P. N. Martinov, A. A. Osipov, A. A. Senin, and A. N. Yudin, JETP Lett. **95**, 326 (2012).
[4] J. I. A. Li, A. M. Zimmerman, J. Pollanen, C. A. Collett, W. J. Gannon, and W. P. Halperin, Phys. Rev. Lett. **112**, 115303 (2014).
[5] E. V. Thuneberg, S. K. Yip, M. Fogelström, and J. A. Sauls, Phys. Rev. Lett. **80**, 2861 (1998).
[6] K. Aoyama and R. Ikeda, Phys. Rev. B **73**, 060504(R) (2006).
[7] C. L. Vicente, H. C. Choi, J. S. Xia, W. P. Halperin, N. Mulders, and Y. Lee, Phys. Rev. B **72**, 094519 (2005).
[8] J. Pollanen, J. I. A. Li, C. A. Collett, W. J. Gannon, and W. P. Halperin, Phys. Rev. Lett. **107**, 195301 (2011).

[9] J. I. A. Li, J. Pollanen, C. A. Collett, W. J. Gannon, and W. P. Halperin, J. Phys. Conf. Ser. **400**, 012039 (2012).
[10] J. I. A. Li, J. Pollanen, A. M. Zimmerman, C. A. Collett, W. J. Gannon, and W. P. Halperin, Nat. Phys. **9**, 775 (2013).
[11] J. Pollanen, K. R. Shirer, S. Blinstein, J. P. Davis, H. Choi, T. M. Lippman, L. B. Lurio, and W. P. Halperin, J. Non-Cryst. Solids **354**, 4668 (2008).
[12] A. M. Zimmerman, M. G. Specht, D. Ginzburg, J. Pollanen, J. I. A. Li, C. A. Collett, W. J. Gannon, and W. P. Halperin, J. Low Temp. Phys. **171**, 745 (2013).
[13] See Supplemental Material at http://link.aps.org/supplemental/10.1103/PhysRevLett.114.105302, which includes Refs. [14–20], for the connection between stress, strain, and anisotropy and details of the tip angle behavior of the frequency shift.
[14] J. Pollanen, Ph.D. thesis, Northwestern University, 2012.
[15] G. E. Volovik, JETP Lett. **63**, 301 (1996).
[16] A. I. Larkin, JETP Lett. **31**, 784 (1970).
[17] Y. Imry and S. Ma, Phys. Rev. Lett. **35**, 1399 (1975).
[18] G. E. Volovik, J. Low Temp. Phys. **150**, 453 (2008).
[19] W. F. Brinkman and H. Smith, Phys. Lett. **51**, 449 (1975).
[20] J. A. Sauls and P. Sharma, Phys. Rev. B **68**, 224502 (2003).
[21] D. Rainer and J. W. Serene, Phys. Rev. B **13**, 4745 (1976).
[22] J. W. Serene and D. Rainer, Phys. Rev. B **17**, 2901 (1978).
[23] G. Gervais, K. Yawata, N. Mulders, and W. P. Halperin, Phys. Rev. B **66**, 054528 (2002).
[24] W. P. Halperin, H. Choi, J. P. Davis, and J. Pollanen, J. Phys. Soc. Jpn. **77**, 111002 (2008).
[25] H. Choi, J. P. Davis, J. Pollanen, T. M. Haard, and W. P. Halperin, Phys. Rev. B **75**, 174503 (2007).
[26] J. I. A. Li, Ph.D. thesis, Northwestern University, 2014.
[27] A. J. Leggett, Rev. Mod. Phys. **47**, 331 (1975).
[28] The free energy difference between the two phases is much smaller than the superfluid condensation energy [29].
[29] J. E. Baumgardner and D. D. Osheroff, Phys. Rev. Lett. **93**, 155301 (2004).
[30] V. V. Dmitriev, D. A. Krasnikhin, N. Mulders, A. A. Senin, G. E. Volovik, and A. N. Yudin, JETP Lett. **91**, 599 (2010).
[31] J. Elbs, Y. M. Bunkov, E. Collin, H. Godfrin, and G. E. Volovik, Phys. Rev. Lett. **100**, 215304 (2008).